

A Coupled SFM-ASCRIBE Model to Investigate the Influence of Emotions and Collective Behavior in Homogeneous and Heterogeneous Crowds

Yassine Lamrhary^{1,2} · Aissam Jebrane¹ · Pierre Argoul³ · Adnane Boukamel¹ · Abdellah Hamdaoui²

¹ Centrale Casablanca, Complex Systems and Interactions Research Center, Ville Verte, Bouskoura, Morocco

E-mail: yassine.lamrhary@centrale-casablanca.ma, aissam.jebrane@centrale-casablanca.ma, adnane.boukamel@centrale-casablanca.ma

² Laboratoire d'Ingénierie Et Matériaux LIMAT, Faculté Des Sciences Ben M'Sik, Hassan II University of Casablanca, Casablanca, Morocco

E-mail: hamdaoui.abdellah@gmail.com

³ Université Gustave Eiffel, MAST-EMGCU, Marne-la-Vallée, France

E-mail: pierre.argoul@univ-eiffel.fr

Received: 7 October 2023 / Last revision received: 19 December 2023 / Accepted: 16 January 2024

DOI: [10.17815/CD.2024.147](https://doi.org/10.17815/CD.2024.147)

Abstract The understanding of crowd behavior dynamics holds immense significance in ensuring public safety across a range of situations, including emergency evacuations and large-scale events. Our research focuses on two primary objectives: investigating the impact of emotions on crowd movement and gaining valuable insights into collective behavior within crowds. To achieve this, we present a coupled model, incorporating an enhanced ASCRIBE model with an agent displacement model. We introduce heterogeneity into our model by incorporating specific mobility laws for different categories of panicked crowds, considering the influence of emotions on both speed and direction. Through numerical simulations, we analyze the model's parameters, observe the behavior of uniform crowds, and explore the collective dynamics within diverse crowds. By conducting comprehensive simulations and analyses, the findings from this study can contribute to the development of more effective crowd management strategies and emergency evacuation protocols.

Keywords Crowd dynamics · emotional contagion · panic propagation · emergency evacuation · decision making

1 Introduction

For many years, researchers have been focused on the study of crowd behavior in various areas. Understanding how crowds move and behave is crucial, especially in panic situations. Experimental setups, often involving real-world scenarios and controlled environments, have been designed to closely monitor and analyze crowd dynamics such as pushing behaviour [1], bottleneck effects [2] and stop and go waves [3]. In an effort to shed light on the factors influencing human crowd evacuation during such circumstances, scientists have developed various models, focusing on two main categories: macroscopic and microscopic models.

Macroscopic models represent the overall movement of a crowd through a set of differential equations generally based on fluid mechanics. These equations describe the changes in velocity and density at each point in space. Such models effectively showcase the collective behavior of crowds. However, they tend to overlook the specific traits and behaviors of individuals. On the other hand, microscopic models focus on capturing the complex details of how pedestrians move as individuals, by describing their velocities and directions. The social force model (SFM) [4], cellular automata model [5], and lattice gas model [6] are widely recognized as prominent microscopic models. Among them, SFM has gained significant popularity for its simple mathematical formulation, clear physical meaning and good ability of describing the movement process [7], and continues to be enhanced by numerous researchers to attain more accurate outcomes in diverse complex environments. In our previous works [8–10], we developed a 2D discrete model based on SFM model and the theory of non-smooth granular model proposed by Frémond to manage multiple and simultaneous collisions between pedestrians. However, the model is not adapted to deal with pedestrians' emotional changes and to reproduce panic situations. Another practical challenge arises from considering pedestrians as homogeneous rigid particles, as it fails to account for individual variations in the crowd.

Helbing et al. [11] integrated panic factor in both desired speed and desired direction to model herding behaviour during evacuation process. Fu et al. [12] coupled cellular-automata model with the SIRS model while introducing an emotion parameter for susceptible individuals. Cao et al. [13] developed the P-SIS model by combining the OCEAN model and SIS model and coupling it with the SFM. Cornes et al. [14] presented a model of panic propagation process, where many individuals may suddenly switch to an anxious state, that was coupled with the SFM. Other models [15, 16] interested to crowds evacuation in multi-hazard situations. The movements of each individual in their models was determined by modeling the emotion of panic and other features such as physical strength consumption and officers assistance. Zhou et al. [17] proposed an emotion contagion that considers personality traits, emotion state, intimacy, and panic level. Individual emotions can influence the path selection time. Mao et al. [18] presented an emotional contagion-based model that integrates peer decision-making in emergency evacuations, considering factors such as emotion contagion, intimacy-based decision-making, environmental familiarity, and task difficulty. Liu et al. [19] established an emotional contagion model based on information transmission process, enabling the construction of a behavior mechanism for agents taking into account emotional contagion. Cao et al. [20] proposed an

evacuation model that integrates the influence of stress factors on crowd evacuation performance by allowing evacuees to adjust their desired moving speed in response to the surrounding fire event. In Xu et al. [21] paper, the emotional process assumes that pedestrians are influenced by nearby individuals, resulting in the identification of two emotional states (negative and positive) that determine the pedestrian's desired speed. To simulate how people in panic follow their leader and escape, Mao et al. [22, 23] developed a novel crowd behavior simulation method that incorporates the Leader-Follower model, an emotional model, and an enhanced SFM that considers forces within and among groups. Xiao et al. [24] explored the dynamic emotional perception influenced by personal walking speed and others in the domain, and integrated emotional contagion into an improved cellular automata model. Li et al. [25] proposed a model that incorporates three crisis factors (residence time, crowd density, and exit distance) directly impacting the desired speeds of pedestrians, resulting in varying levels of emotion. Niu et al. [26] presented a new model for emergent evacuation with assailants, utilizing the Susceptible-Infected-Susceptible model. The panic factor was defined as a function of density and the distance between pedestrians and the assailant, directly influencing their speed.

Many works aimed integrate heterogeneity in crowd models. Guo et al. [27] proposed a heterogeneous lattice gas model for studying pedestrians' evacuation processes, considering critical damage force, local density, and exit congestion as factors in the updating rule. Cao et al. [20] proposed an improved SFM to model the raised stress created by the physical threat of fire, incorporating the variation of evacuees' stress levels. Hrabak et al. [28] introduced parameters into the Floor-Field model such as velocity, aggressiveness, and sensitivity to occupancy as heterogeneity features. Li et al. [29] developed a behavior-based cellular automata model that introduced aggressiveness as an internal state, affecting motion characteristics and pedestrians' behavior preferences. Wu et al. [30] extended an existing model to simulate the evacuation of mixed crowds, including disabled pedestrians, to achieve a more realistic representation. Ma et al. [7] analyzed desired speed within the SFM, where nine models of desired speed are examined, highlighting the impact of heterogeneity on model performance. Wu et al. (2021) developed a pedestrian heterogeneity-based social force model (PHSFM) by incorporating physique and mentality coefficients, introducing a heterogeneous coefficient that modifies the self-driven force. Later, the PHSFM model was improved to the behavioral heterogeneity-based social force model (BHSFM) [31], by explicitly considering panic parameters, physique coefficients, and other emergency environment and individual difference factors.

Most of the aforementioned models have not taken into account the phenomenon of emotional contagion that occurs during panic situations. Even for the models that do consider panic factors, the integration of the contagion process is lacking, with the temporal evolution of the panic parameter relying solely on the speed of movement. However, the incorporation of emotional contagion is an important aspect that has been overlooked. By considering the influence of emotional contagion, we may capture the complex dynamics and behaviors exhibited by crowds during emergencies.

In this paper, Section 2 provides an introduction to the displacement model that was developed earlier. Moving on to Section 3, we present an improved ASCRIBE model that effectively captures the emotional dynamics of individuals and controls the spread of

panic within a crowd. Section 4 introduces mobility laws specific to different categories of panicked crowds, taking into account the impact of emotions on both speed and direction. Finally, in Section 5, we conduct numerical simulations to analyze the parameters of the coupled model, examine the behavior of uniform crowds, and explore the collective dynamics within diverse crowds.

2 A modified SFM of pedestrian movement

The movement of individuals within specific locations is characterized using a social force formalism. This framework considers each pedestrian as a particle that experiences various forces. By employing Newton's second law of dynamics, we can calculate the displacement of pedestrians over time. The development of SFM originated from the work of Helbing and Molnar [4] and has since been applied to analyze pedestrian flows in a range of scenarios, including bottleneck entrances and panic situations. In our study, we utilize a previously validated version of SFM that accurately captures the movement of individuals within crowded environments [32, 33]. We describe the movement of each individual as follows:

2.1 At a distance interactions

$$m_i \frac{d\mathbf{v}_i}{dt} = \mathbf{f}_i^{self} + \sum \mathbf{f}_{ij}^{soc} + \sum \mathbf{f}_{iW}^{obs}, \quad (1)$$

Equation 1 presents the formulation governing the smooth evolution of the system, which takes into account various factors influencing individual movement. In this equation, m_i represents the mass of the individual, \mathbf{v}_i denotes their velocity vector, and \mathbf{f}_i^{self} corresponds to the self-driven force acting on the individual. This force accounts for the adjustment of pedestrian movement speed to attain the desired velocity $v_{d,i}$ and the desired direction $\mathbf{e}_{d,i}$, as expressed by:

$$\mathbf{f}_i^{self} = m_i \frac{v_{d,i} \mathbf{e}_{d,i} - \mathbf{v}_i}{\tau_i}, \quad (2)$$

τ_i is the relaxation time which represents the needed time for the pedestrian velocity to adapt to the desired speed.

We now incorporate the social psychological force exerted by pedestrians towards each other. The initial formulation of this force was introduced by Helbing and Molnar [4]. However, recent studies have modified this force to account for avoidance behavior between neighboring individuals and enable them to maintain a desired distance [32]. \mathbf{f}_{ij}^{soc} is the social psychological force between the i -th and j -th individuals, given as follows:

$$\mathbf{f}_{ij}^{soc} = \begin{cases} A_{soc} \exp\left(\frac{d_{ij} - d_{soc}}{\beta_{soc}}\right) \mathbf{e}_{ij}, & \text{if } d_{ij} < d_{soc} \\ 0, & \text{elsewhere} \end{cases}, \quad (3)$$

A_{soc} represents the magnitude of the social psychological force exerted between pedestrians, d_{ij} denotes the distance between two pedestrians, i and j , d_{soc} corresponds to the

desired interpersonal distance, indicating the distance individuals tend to maintain between themselves, and β_{soc} characterizes the falloff length of the social psychological force, governing how quickly the force diminishes with increasing distance.

Moreover, the interactions of each individual with the surrounding environment are accounted by using the force \mathbf{f}_{iw}^{obs} . This force is an exponential repulsive force that intensifies as an individual approaches walls or other obstacles, reflecting the inherent tendency to avoid collisions and maintain a safe distance:

$$\mathbf{f}_{iw}^{obs} = \begin{cases} A_{obs} \exp\left(\frac{d_{iw}-d_{obs}}{\beta_{obs}}\right) \mathbf{e}_{iw}, & \text{if } d_{iw} < d_{obs} \\ 0, & \text{elsewhere} \end{cases}, \quad (4)$$

where A_{obs} denotes the magnitude of the psychological force between a person and a wall. The distance separating the individual from the wall is represented by d_{iw} . Each individual strives to maintain a distance of d_{obs} from the wall. β_{obs} characterizes the falloff length of the social psychological force, governing how quickly the force diminishes with distance from the wall. Lastly, \mathbf{e}_{iw} is the normal vector that points from the wall towards pedestrian i .

2.2 Contact management

When contact is detected, the velocities of the colliding particles become discontinuous. Therefore, interior percussions \mathbf{p}_i^{int} and exterior percussions \mathbf{p}_i^{ext} are introduced and used to calculate the velocity after the shock, following the equation:

$$m_i (\mathbf{v}_i^+ - \mathbf{v}_i^-) = -\mathbf{p}_i^{int} + \mathbf{p}_i^{ext} \quad (5)$$

\mathbf{v}^- and \mathbf{v}^+ are the agent's velocities before and after a collision. The interior percussions \mathbf{p}_i^{int} take in account the dissipative interactions between the colliding particles and the reaction forces that permit the avoidance of overlapping among particles. It is expressed using a pseudo-potential of dissipation Φ as:

$$\mathbf{p}^{int} \in \partial\Phi\left(\mathcal{D}\left(\frac{\mathbf{v}^+ + \mathbf{v}^-}{2}\right)\right) \quad (6)$$

where $\mathcal{D}(\mathbf{v}) = (\Delta(\mathbf{v}), \Delta^*(\mathbf{v}))$, $\Delta(\mathbf{v})$ represents the vector containing all the velocities of deformation of all the particles in contact, and $\Delta^*(\mathbf{v})$ represents the vector containing all the at-a-distance deformation velocities of the particles belonging to groups. The operator ∂ is the sub-differential that generalizes the derivative for convex functions.

The convex function Φ is defined as the sum of two pseudo-potentials [10]:

$$\Phi = \Phi^d + \Phi^r, \quad (7)$$

where:

- Φ^d characterizes the dissipative interior percussions given by:

$$\Phi^d(\mathcal{D}(\mathbf{v})) = \frac{1}{2} \sum_{1 \leq i \leq j \leq N} K_n \left({}^t \Delta_{ij}(\mathbf{v}) \cdot \mathbf{e}_{ij}^n \right)^2 \quad (8)$$

The dissipation coefficient K_n for the normal component of dissipative percussion characterizes the inelastic nature of the collisions between particles; an infinite value of K_n implies a perfectly elastic collision.

- Φ^r characterizes the reactive interior percussions, which ensure non-interpenetration between particles. It is equal to zero if the contact is not maintained after the collision (that is, $\Delta_{ij}(\mathbf{v}^+) \cdot \mathbf{e}_{ij}^n < 0$) and positive if contact is maintained after collision (i.e., $\Delta_{ij}(\mathbf{v}^+) \cdot \mathbf{e}_{ij}^n = 0$) where \mathbf{e}_{ij}^n is the unit vector pointing from agent i to agent j . These conditions allow us to write:

$$\Phi^r = I_{\mathbb{R}^-} \left(\Delta_{ij}(\mathbf{v}^+) \cdot \mathbf{e}_{ij}^n \right) \quad (9)$$

The introduced system leads to a constrained minimization problem:

$$\mathbf{X} = \arg \min_{\mathbf{Y} \in \mathbb{R}^{3N_c}} \left[{}^t \mathbf{Y} \mathbf{M} \mathbf{Y} + \Phi(\mathcal{D}(\mathbf{Y})) - {}^t (2\mathbf{v}^- + \mathbf{M}^{-1} \mathbf{p}^{ext}) \mathbf{M} \mathbf{Y} \right] \quad (10)$$

with $\mathbf{Y} = \frac{\mathbf{v}^+ + \mathbf{v}^-}{2}$ and N_c the number of pedestrians in contact.

3 Emotional contagion model

In this paper, we distinguish between two extreme behaviors: terrified or stressed agents who transmit negative emotions, and calm agents who transmit positive emotions. Depending on their personality traits, the other agents have an intermediate action and contribute positively or negatively to the spread of panic. To accomplish this, we opt for a solicitation-response paradigm, in which multiple reactions can occur depending on the agent's response to a solicitation applied by his environment (other agents, stimulus, etc.)

Let's call E_i the emotional intensity of an agent i ; A normalized dimensionless variable. The value of E_i allows to assign different emotional states: calm if $E_i = 0$, anxiety if $E_i \in (0, 0.4]$, panic if $E_i \in (0.4, 0.8]$, and hysteria if $E_i \in (0.8, 1]$ [34]. We note E_i^a the local average emotional intensity in an agent's neighborhood i , which is evaluated based on the elementary solicitations exerted on agent i by agents j , with $j \neq i$.

Consider a crowd of n agents. The evolution of the emotional intensity of an agent $2 \leq i \leq n$ is governed by the following dynamic system:

$$\frac{dE_i}{dt} = \beta_i E_i^a (1 - E_i) + (1 - \beta_i) E_i (E_i^a - 1) \quad (11)$$

where $\beta_i \in [0, 1]$ is a resilience parameter that refers to how an agent interprets a stimulus. The term $E_i^a (1 - E_i)$ is positive and corresponds to a population that tends to be panicked with a speed E_i^a , whereas the term $E_i (E_i^a - 1)$ is negative and used to describe the calm population. The other behaviours can be generated by linearly combining these

two regimes; If $\beta_i > 0.5$, the agent has a negative perspective and is more likely to increase his emotional intensity. The agent has a strong resilience and tends to lower his emotional intensity if $\beta_i < 0.5$. If $\beta_i = 0.5$, the agent has a moderate resilience and adjusts his emotional intensity to the average emotional intensity E_i^a .

The average local emotional intensity E_i^a refers to the applied environment's solicitation on agent i . It is affected by a variety of elements, including the expressivity of other agents, their velocities and fields of vision, the quality of the domain and the type of the stimulus. To define it, We propose using the following formula:

$$E_i^a = \sum_{\substack{j=1 \\ j \neq i}}^n \frac{g_{ij}}{\sum_{\substack{k=1 \\ k \neq i}}^n g_{ik}} E_j \quad (12)$$

with $g_{ij}E_j$ designates an elementary solicitation of agent j , and g_{ij} reflects the amplitude of this elementary solicitation, which can model the expressiveness of the agent j , as well as the domain's quality. Intuitively, with a large distance between two agents, it becomes hard to clearly define actions and expressions. Consequently, the elementary solicitation amplitude is impacted by the distance d_{ij} between these two agents. Thus, we define the amplitude of the elementary solicitation as a radial function $g_{ij} = \frac{1}{2}(1 + \cos(\frac{d_{ij}}{d_0}\pi))$ if $d_{ij} < d_0$ else 0, with d_0 is a characteristic radius to model the scope of the contagion impacted by agent j .

4 Constitutive laws of emotions-velocities

Our modeling approach is based on insights from psychological studies [35], which have identified four distinct categories in which agents tend to fall after experiencing a panic situation: 1) Stupor: where persons are in a state of stupefaction caused by danger in which the brain itself may decide that the best chance of survival is not to move at all. 2) Agitation: where persons have an intense energy that cannot channel effectively, start to make large gestures, coming and going in a disordered way. 3) Panic Flight: where persons instinctively run away or towards danger without paying attention to everything around. 4) Adapted: persons who evacuate in an orderly fashion. They may obey orders, or they may help others. Building upon these definitions, we have developed mobility laws for each category, taking into account the influence of emotions on both speed and direction, which we have summarized in Table 1.

In previous researches [11, 14–16], authors have employed a linear relationship to describe the connection between emotions and speed. However, unlike the linear relationship, which maintains a constant slope and results in abrupt transitions, the sigmoid function offers a smooth and continuous transition from one value to another as the input changes. This characteristic makes the sigmoid function a more suitable choice for capturing the complex phenomenon of emotions-velocities dynamics, which cannot be adequately represented by a simple linear function. Therefore, we propose a novel formula that adopts a logistic form for modeling changes in speed, taking into account the intricate nature of the emotions-velocities relationship:

$$v_{d,i} = f_{k,v_{lim}}(E_i) = \tilde{g}_k(E_i)(v_{lim} - v_0) + v_0 \quad (13)$$

\tilde{g}_k represents the normalized version of the logistic function g_k , ensuring its values lie within the interval $[0, 1]$:

$$g_k(x) = \frac{1}{1 + \exp(-x - k)} \quad (14)$$

The variable v_0 represents the typical speed exhibited by an agent when they are in a calm state. On the other hand, v_{lim} denotes the maximum speed that an agent can attain when they are fully panicked. The coefficient k governs how sensitive the agent's speed is to changes in their emotional state. Higher values of k amplify the agent's desired speed even with relatively low levels of emotional intensity, causing the agent to converge quickly towards the maximum speed. In simpler terms, even a slight increase in emotional intensity can prompt the agent to desire a significant increase in speed. Conversely, lower values of k result in the desired speed being less affected by minor changes in emotional state and a slower convergence towards the maximum speed. In other words, the agent does not have a strong inclination to run at high speed unless the emotional intensity reaches a considerable level.

Regarding the decision-making process for choosing a direction, we provide the agent with the ability to select from multiple directions based on their respective category. The following definitions apply:

- **Direction to the closest exit:** To choose their path, individuals consider all the pedestrians and the congestions that are visible to them. To model this medium navigation behavior, floor fields are used [32]. The dynamic floor field $D(x, t)$ is constructed by solving the following Eikonal equation:

$$\begin{aligned} V(\mathbf{x}, t) \|\nabla D(\mathbf{x}, t)\| &= 1 \\ D(\mathbf{x}, t) &= 0 \end{aligned} \quad (15)$$

$D(\mathbf{x}, t)$ represents the expected travel times giving the fastest path displacement strategy and $V(\mathbf{x}, t)$ is the estimated travel speed. The static floor field has been already used in our model only for $V(\mathbf{x}, t) = 1$ and the shortest path strategy was successfully modeled [36]. For simplicity, we choose this value for the rest of the paper. The direction is then obtained by: $\mathbf{e}_i^{\text{exit}} = \frac{\nabla D(\mathbf{x}, t)}{\|\nabla D(\mathbf{x}, t)\|}$.

- **Direction to zones with low emotional intensity:** A natural response of an agent to avoid zones with high emotional intensity increases panic and causes considerable physical and mental damage [15]. We constitute a dynamic floor field based on the emotional intensity E_i that we interpolate in space to obtain a continuous field. The direction is then obtained by: $\mathbf{e}_i^{\text{emotion}} = -\frac{\nabla E(\mathbf{x}, t)}{\|\nabla E(\mathbf{x}, t)\|}$.
- **Direction to zones with low density:** In normal situations, people tend to avoid high density zones while walking due to the increased risk of injury or accidents

[37]. In a panic situation context, being in an overcrowded areas increases stress and anxiety, as well as decreases reaction times in the event of an emergency. We constitute a dynamic floor field based on the density ρ_i defined as the number of agents on the radius of $2m$ that we interpolate in space to obtain a continuous field. The direction is then obtained by $\mathbf{e}_i^{\text{density}} = -\frac{\nabla\rho(\mathbf{x},t)}{\|\nabla\rho(\mathbf{x},t)\|}$.

- Direction taken by the majority: People tend to follow the direction of others while walking due to a phenomenon known as herding behaviour. This behavior is likely due to a desire for predictability and familiarity. People are more comfortable when they know what to expect from their environment and those around them. Following the same direction as others provides this sense of security and familiarity. Additionally, following the same direction as others can help people save energy and time since they don't have to think about which way they should go. We choose to represent this behavior by the mean direction of neighbors existing in a certain radius [15]: $\mathbf{e}_i^{\text{avg}} = \sum_{j \in \text{neighbors}(i)} \mathbf{e}_j$.

Class	Sensitivity k	Limit velocity v_{lim}	Desired direction	Resilience β_i	Initial emotional intensity
Stupor	4	0	$\mathbf{e}_{d,i} = \mathbf{1}_{\rho_i < \rho_{th}} \mathbf{e}_i^{\text{exit}} + (1 - \mathbf{1}_{\rho_i < \rho_{th}}) \mathbf{e}_i^{\text{avg}}$	Random(0.5, 1)	Random(0.4, 1)
Agitation	4	v_{max}	$\mathbf{e}_{d,i} = \begin{cases} \mathbf{e}_i^{\text{exit}} & \text{during } T_1 \\ \mathbf{e}_i^{\text{random}} & \text{during } T_2 \end{cases}$	Random(0.5, 1)	Random(0.4, 1)
Panic flight	3	v_{max}	$\mathbf{e}_{d,i} = \mathbf{1}_{E_i < E_{th}} \mathbf{e}_i^{\text{exit}} + (1 - \mathbf{1}_{E_i < E_{th}}) \mathbf{e}_i^{\text{emotion}}$	Random(0.5, 1)	Random(0.4, 1)
Adaptation	2	v_{max}	$p = \text{argmin} \left(\frac{d_{is}}{d_{\text{max}}}, \frac{\rho_i}{\rho_{\text{max}}}, \frac{E_i}{E_{\text{max}}} \right)$ $\mathbf{e}_{d,i} = \begin{cases} \mathbf{e}_i^{\text{exit}} & \text{if } p = 1 \\ \mathbf{e}_i^{\text{density}} & \text{if } p = 2 \\ \mathbf{e}_i^{\text{emotion}} & \text{if } p = 3 \end{cases}$	Random(0, 0.5)	Random(0, 1)

Table 1 A summary of panicked crowd classes and their characterisations.

Table 1 provides a summary of panicked crowd classes with their respective emotional and mobility attributes. The symbol $\mathbf{1}$ denotes the characteristic function (meaning that for a given subset A, $\mathbf{1}_A(x) = 1$ if x is an element of A, and $\mathbf{1}_A(x) = 0$ if it is not). As detailed in the table 1, the behavior of agents in the stupor class is characterized by alternating actions: they either move towards the nearest exit or align with the majority's direction, the choice of which depends on the local density ρ_i value compared with a

threshold ρ_{th} . The stupor class is also marked by a heightened response to emotional intensity, as evidenced by a relatively high value of the coefficient k . Additionally, agents in this class become immobile in situations of extreme panic, leading to a zero limit speed value. In contrast, agents in the agitation class switch between heading towards the nearest exit for a set duration T_1 , and then adopting a random direction for a subsequent period T_2 . This class is defined by both high sensitivity and a high limit speed. The panic flight class involves agents dynamically alternating between moving towards the nearest exit and moving towards areas of low emotional intensity, with the choice influenced by their current emotional intensity value compared with a threshold E_{th} . Compared to the agitation class, the panic flight class is slightly less sensitive but also exhibits a high limit speed. Finally, the adaptation class exhibits an oscillated behavior between the nearest exit, areas of low density, and zones with low emotional intensity. Their decision-making process involves the computation of a utility function that takes into account the distance to the exit d_{iS} , the local density, and the emotional intensity. To ensure comparability, these parameters are normalized using their maximal values d_{max} , ρ_{max} , and E_{max} , aligning them within a consistent range. This class is characterized by the lowest sensitivity due to their capacity of self-control.

5 Numerical simulations

This section studies the effect of model's parameters, the behaviour of homogeneous crowd constituted by each class, and the response of an heterogeneous crowd.

5.1 Experiment setup

The parameter settings of experimental evacuation scenario is the following: 200 agents in a geometry configuration of a square compartment room with the size of 20m \times 20m with a 1m wide exit is set up for this study. Table 2 summarizes all parameters in the model with the considered values in the simulation. The evacuation process is illustrated in figure 1, where plot a heat map of the local emotional intensity in each point of the space.

5.2 Impact of resilience on emotional contagion

The variation of an individual's emotional intensity is influenced by a combination of two fundamental elements: the degree of external stimulation provided by the surrounding environment, denoted as the local average emotional intensity E_i^a , and the personal resilience of the agent β_i , which encapsulates distinctive attributes of their character and disposition. For a supposedly constant local average emotional intensity, the analytical solution of equation 11 is given by:

$$E_i(t) = (E_{i,0} - E_{i,\infty}) \exp\left(\frac{-t}{\tau_i}\right) + E_{i,\infty} \quad (16)$$

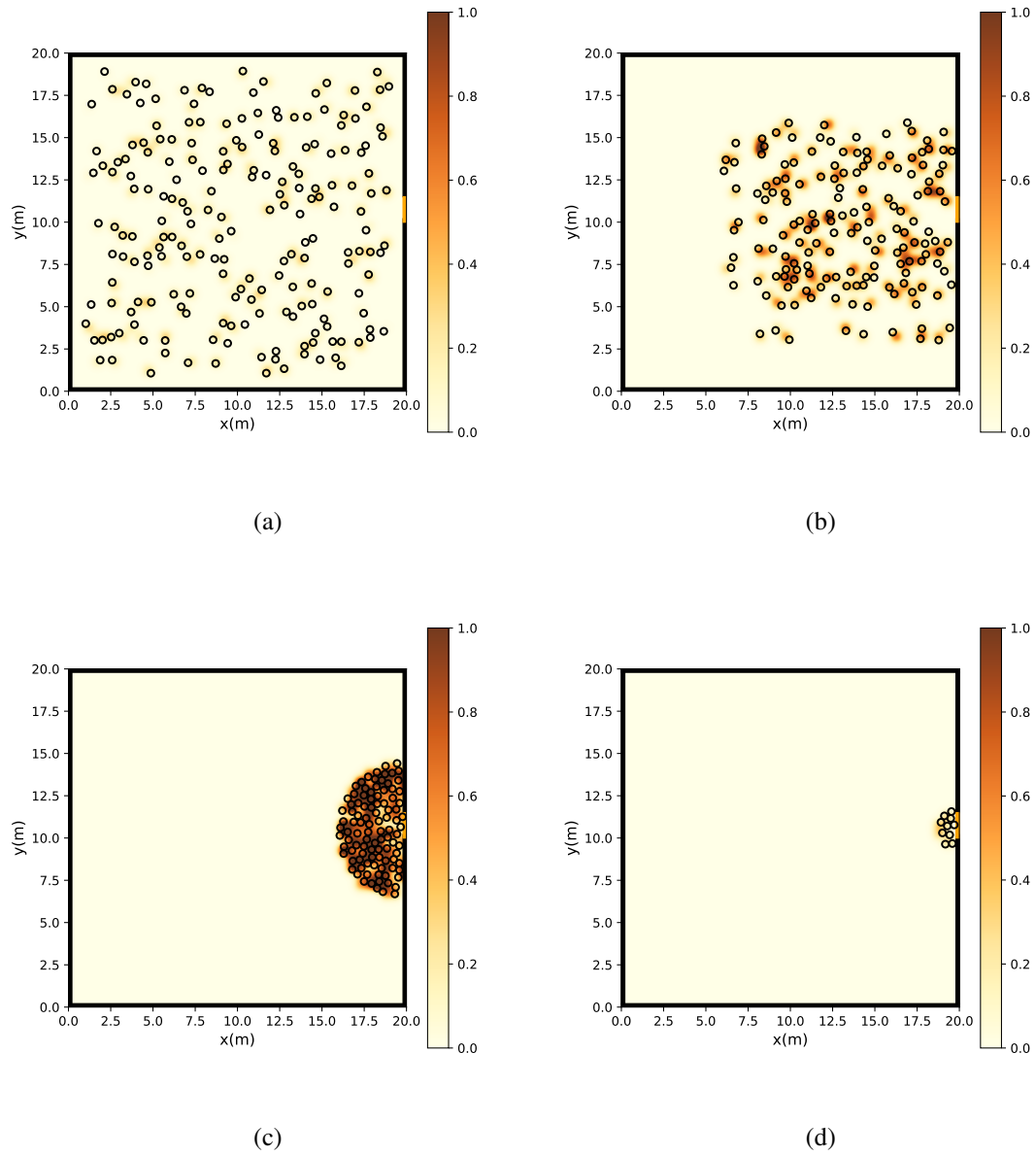


Figure 1 Snapshots of evacuation with 200 evacuees at various time steps a) at $t = 0s$ b) at $t = 5s$ c) at $t = 20s$ d) at $t = 50s$.

Parameter	Interpretation	Value
m_i	Mass of an individual agent	80 kg [11]
r_i	Radius of an individual agent	0.2 m [32]
τ_i	Relaxation time	0.5 s [11]
A_{soc}, A_{obs}	Social and obstacle force amplitudes	2000 N [11]
β_{soc}, β_{obs}	Social and obstacle interaction factors	0.08 m [11]
d_{soc}, d_{obs}	Social force interaction distance	1 m
K_n	Normal coefficient for the tangential component of percussion	10^5 kg [32]
d_0	Characteristic radius for the emotional model	2 m
v_0	Speed value in calm state	1.34m [32]
v_{max}	Maximal speed in panicked state	3 m/s [16]
ρ_{th}	Density threshold for switching direction	2 p/m^2
E_{th}	Emotional intensity threshold for switching direction	0.4 [34]
ρ_{max}	Maximal density value	5 p/m^2 [38]
E_{max}	Maximal emotional intensity value	1
d_{max}	Maximal exit distance value	20 m

Table 2 Parameters, their interpretations, and values in the proposed model

with $\frac{1}{\tau_i} = (1 - \beta_i) - (1 - 2\beta_i)E_i^a$ and $E_{i,\infty} = \tau_i\beta_iE_i^a$. The asymptotic behavior of an agent's emotional state remains unaffected by their initial emotional intensity in response to a stimulus. Instead, it is primarily determined by two key factors: the individual's resilience β_i , and the average local emotional intensity within their environment E_i^a . To illustrate this, figure 2 provides the limit emotional intensity reached by an agent, based on varying values of the parameter β_i and the average local emotional intensity E_i^a . The graph showcases the relationship between these two factors and their influence on the agent's ultimate emotional state. We note that in our analysis, two singular points, namely $(\beta_i, E_i^a) = (0, 1)$ and $(\beta_i, E_i^a) = (1, 0)$, have been excluded. These points are characterized by undefined values of the parameter τ_i , resulting in the agent maintaining their initial emotional value over time. Therefore, we focus our examination on the remaining parameter space.

When considering a specific value of β_i within the interval $]0, 1[$, the limit of emotional intensity $E_{i,\infty}$ varies in the same direction as the average local emotional intensity E_i^a . This pattern, however, differs depending on whether the agent has a strong or weak resilience. In contrast to agents with strong resilience ($0 < \beta_i < 0.5$), agents with weak resilience ($0.5 < \beta_i < 1$) demonstrate high sensitivity to minor solicitation and are significantly influenced by the emotional atmosphere in their environment. This implies that agents with weak resilience are more susceptible to emotional stimuli and are prone to negative effects from the surrounding emotional context.

Specifically, when β_i is set to 0, the limit emotional intensity $E_{i,\infty}$ is equal to 0. This indicates that agents with a high level of resilience are capable of maintaining a state of calmness regardless of the average local emotional intensity E_i^a . Their strong resilience

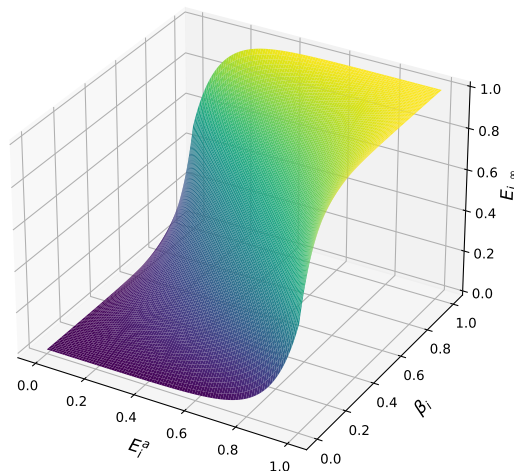


Figure 2 Variation of the limit-emotional intensity $E_{i,\infty}$ of an agent i as a function of its resilience β_i and its average local emotional intensity E_i^a .

shields them from being strongly affected by the emotional atmosphere in their surroundings. Conversely, when β_i is equal to 1, the limit emotional intensity $E_{i,\infty}$ is equal to 1. This signifies that agents with weak resilience experience an extreme panic state, irrespective of the average local emotional intensity E_i^a . Their low resilience makes them highly vulnerable to the influence of their emotional environment, resulting in heightened emotional intensity. Finally, for agents with a resilience parameter of 0.5, the limit emotional intensity $E_{i,\infty}$ is equal to the average local emotional intensity E_i^a . This suggests that agents with moderate resilience fully adopt and mirror the emotional intensity prevailing in their immediate surroundings. Their response to the emotional atmosphere is more balanced compared to those with strong or weak resilience.

By examining the effects of resilience, we gain insights into how different levels of emotional strength or vulnerability shape an agent's emotional state. Agents with strong resilience are better equipped to regulate their emotional responses and remain calm even in emotionally charged environments. On the other hand, agents with weak resilience are highly reactive to emotional stimuli, which can lead to intensified emotional experiences.

5.3 Impact of movement on emotional contagion

This study aims to examine the impact of agents' movement on emotional contagion during crowd evacuation scenarios. Specifically, we compare the propagation of panic within a crowd across different speed values, contrasting it with the static case where agents remain stationary. To assess the influence of movement dynamics, we analyze key indicators including the average emotional intensity and proportion of panicked agents.

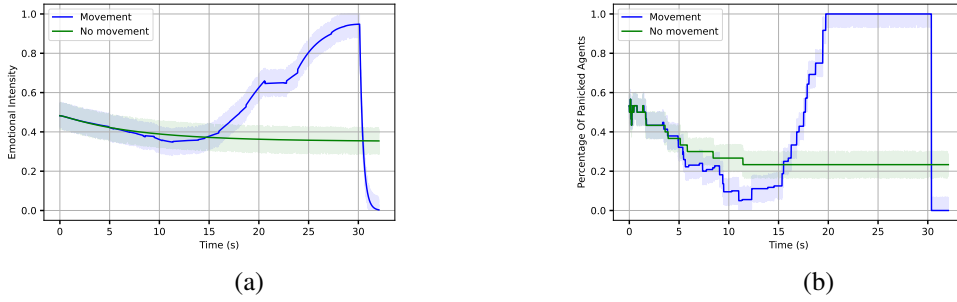


Figure 3 a) Average emotional intensity b) Proportion of panicked agents over time for the dynamic and static cases. The shaded parts refer to the maximum and minimum response obtained by multiple measures.

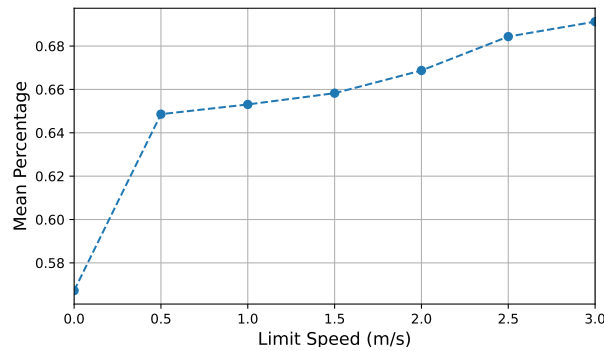


Figure 4 The effect of the limit speed on the mean percentage of panicked agents over the evacuation process

First, we track, as illustrated in figure 3, the average emotional intensity and the proportion of panicked agents over time for the static when agents are immobile, and dynamic cases when agents try to evacuate the room. In the static scenario, where the agents remained immobile, we observed a convergence of the crowd's emotional state towards a stable mean value. This convergence can be attributed to the mathematical formulation of the emotional model employed, in which the dynamic system seeks to establish an equilibrium state based on agents characteristics, resulting in a steady emotional state maintained throughout the duration of the simulation. In contrast, under dynamic conditions, where agents attempt to evacuate the room, we observe an increasing trend in both the average emotional intensity and the proportion of panicked agents over time. These values continue to rise until they reach their peak levels when the agents gathered in close proximity to the exit, decrease until they reached a null value as the last agents evacuate the area.

Secondly, we investigate how different movement speeds affect the average proportion of individuals experiencing panic during the evacuation process. As shown in figure 4, the mean percentage is around 55% when agents are static, drops to 65% when the limit speed is set to 0.5m/s, to arrive to around 70% when the limit speed reaches 3m/s.

The observed trends can be explained by considering the distance between individuals in different scenarios. When individuals remain stationary, there is a considerable distance between them compared to the situation during an evacuation where individuals congregate near the exit, resulting in minimal distances between them. The close proximity during the evacuation facilitates the spread of emotions, leading to a higher proportion of individuals experiencing panic. Furthermore, as the maximum speed increases, individuals spend more time in close proximity to the exit, providing ample opportunity for panic to spread easily among them.

5.4 Impact of environment on emotional contagion

To comprehensively understand the phenomenon of emotional contagion, it is crucial to consider how environmental factors affect the intensity of panic. Our current model primarily focuses on the impact of emotions on speed. However, for this particular section, we will explore the reverse effect, namely how speed influences emotions. Additionally, in this part of our study, we will not engage with the concept of crowd repartition and will instead consider a homogeneous crowd. This approach allows for a clearer analysis of the basic dynamics at play. The exploration of how speed impacts emotions across the four identified classes is a complex topic that warrants an in-depth investigation. We plan to dedicate a separate paper to this subject, ensuring a thorough and focused examination.

In order to quantify the influence of speed on emotional responses, we propose to link the emotional intensity of an individual to the gap between their actual speed and their desired speed. This relationship is mathematically represented as follows:

$$E_i(t) = 1 - \frac{v_i(t)}{v_{i,d}} \quad (17)$$

This formulation aligns with the perspective introduced by Helbing in [11]. According to this model, when an individual's actual speed is close to their desired speed, the emotional intensity decreases, implying a low level of panic. Conversely, if the actual speed is much lower than the desired speed (for instance, due to crowding or obstacles), the emotional intensity increases, indicating a higher level of panic or stress.

The experimental design of our study, as depicted in figure 5, involves a designed space measuring 25 meters in length and 10 meters in width, partitioned into two sections. The first section is a rectangular room measuring 15m in length. Adjacent to this is a corridor that extends for 5m in length, having an exit at its end. The width of the corridor, represented as b , is the key variable in this setup. The objective of our research is to analyze how the width b influences the overall emotional state of the crowd. The crowd density is estimated as $2p/m^2$, and supposed initially in calm state, i.e. $\forall i : E_i(t = 0) = 0$.

The figure demonstrates that changes in the corridor width parameter b substantially influence the emotional intensity among the crowd. Specifically, larger b values indicate a wider corridor, facilitating smooth and uninterrupted evacuation for pedestrians, allowing them to move at a velocity close to their preferred speed. This results in a gradual decrease in emotional intensity over time. Conversely, smaller b values suggest a narrower corridor,

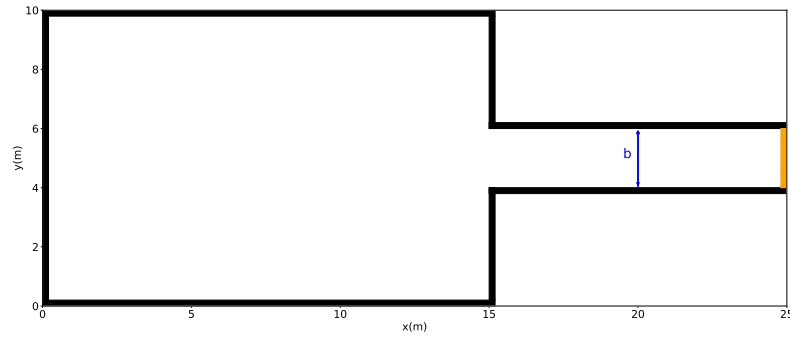


Figure 5 Experimental design to study the environment impact on emotions

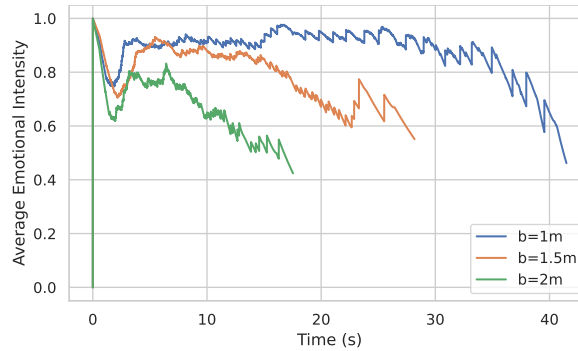


Figure 6 Impact of corridor width on the overall emotional intensity of the crowd

leading to challenging and interrupted evacuation due to blockages, causing pedestrian velocities to deviate significantly from their desired speeds. As a result, the level of emotional intensity stays elevated throughout the period.

5.5 Impact of speed choice on evacuation process

At this stage, we focus our study on the impact of speed choice, specifically the speed limit that an agent reaches when he is fully panicked v_{lim} on evacuation process and the sensitivity of agents speed to emotional changes k .

The arching effect is a phenomenon that occurs during the process of evacuation, where a crowd forms a structure resembling to an arch. In our study, we monitored the size of this arch-shaped structure over time while adjusting the speed limit allowed for the individuals in the crowd. The results depicted in the figure 7 demonstrate that when the maximum speed allowed is set for normal speed $1m/s$, the arch is formed with a maximum radius of 4 meters and diminishes quickly, indicating a smooth evacuation process. However, as the maximum speed allowed increases, the arch becomes larger, reaching a maximum radius close to 5 meters, and the decrease in size becomes much slower, which refers to a clogging effect. In fact, when all individuals within a crowd move at a high speed, they tend to reach the exit simultaneously. This simultaneous arrival leads to an increased density of agents near the exit. Consequently, the flow rate of movement through this restricted zone diminishes, making it more difficult for individuals to traverse out of the

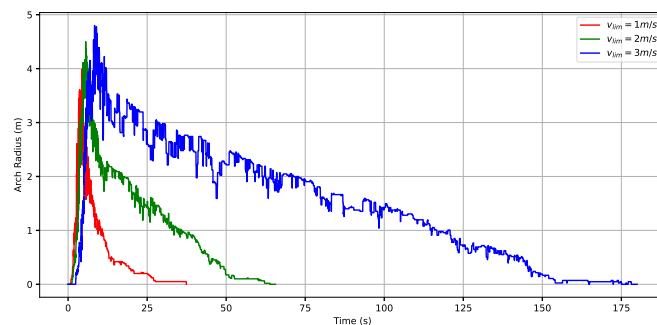


Figure 7 Variation of the arch-shaped radius over time for different speed limit values

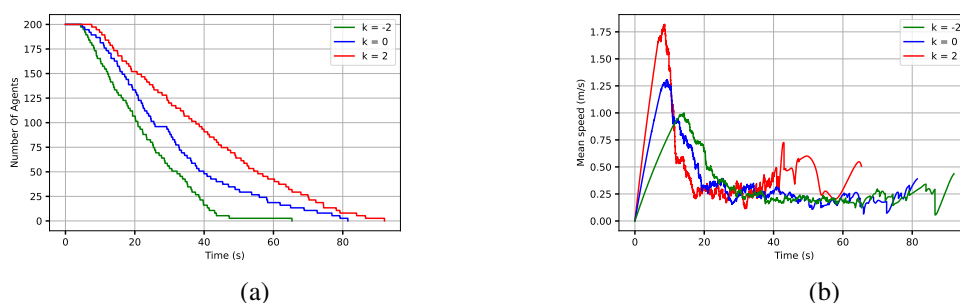


Figure 8 Effect of parameter k on the evacuation process: a) Number of agents remaining in the geometry at each time of the simulation for different values of the parameter k b) Average crowd speed at each time of the simulation for different values of the parameter k .

room.

In addition to the previous factor, the choice of speed in the evacuation process is also influenced by an important parameter referred to as the coefficient k . This coefficient governs the sensitivity of agent speed to emotional changes. To investigate the influence of this parameter on crowd evacuation, we examine two key metrics: the number of agents remaining within the designated geometry and the average speed of the crowd as functions of time for various values of the parameter k , as illustrated in figure 8.

The rate of change of the number of agents remaining in the geometry is influenced by the value of the coefficient k . When k is set to high values, the slope of this variation is more pronounced, indicating a more significant reduction in the number of agents over time. However, as k decreases, the slope becomes less steep, implying a weaker decrease in the number of remaining agents. In parallel, the effect of k on the average speed of the crowd demonstrates the same relationship. For low values of k , there is a notable peak in the average speed, indicating a rapid increase in velocity. As k increases, this peak becomes less pronounced, and the average speed of the crowd experiences a smaller increase.

In fact, the parameter k plays a crucial role in determining the desired speed of individual agents and their sensitivity to emotional changes. Lower values of k indicate a lower sensitivity to emotions, implying that even with high levels of panic intensity,

an agent will move at a moderate speed without immediately reaching their maximum desired velocity. This gradual transition in speed facilitates a smooth and efficient evacuation process, leading to faster overall evacuation times. In contrast, higher values of k suggest a heightened sensitivity to emotions. This means that even with relatively low panic intensity levels, an agent will quickly reach their maximum desired speed. This abrupt transition in speed can result in congestion and slower evacuation rates, leading to a clogging effect.

5.6 Homogeneous crowd behaviour

In panicked crowds, it is essential to examine how individuals in similar crowds respond to stress and fear to better understand collective behavior. By exploring how individuals in similar crowds react, we can gain valuable insights into crowd behavior as a whole. This section aims to emphasize the importance of studying homogeneous crowd behavior in panic situations.

5.6.1 Emotional Intensity

Firstly, we examine the changes in the overall intensity of emotions over time, as shown in figure 9. Among the different categories of emotions, the agitation class exhibits the highest level of panic, showing a significant upward trend. It is followed by the panic flight class, which also experiences an increase in panic levels. The stupor class, on the other hand, demonstrates a relatively lower level of panic compared to the previous two classes. The adapted class, in contrast, exhibits the lowest level of panic, and there is a gradual decrease in panic levels until reaching the calm state.

In fact, individuals belonging to the agitation and panic flight classes display less concern for maintaining distance during the evacuation process. This lack of attention to distancing measures can contribute to the easier occurrence of the contagion phenomenon. Conversely, individuals in the stupor class tend to follow the average direction, thereby increasing the likelihood of contagion. In contrast, individuals in the adapted class demonstrate greater attention to maintaining distance. Additionally, they actively avoid areas with high levels of emotional intensity. These actions contribute to the suppression of the contagion phenomenon, as individuals in the adapted class are better equipped to prevent its spread.

5.6.2 Average Speed

Next, we study the variations in average speed over time, as depicted in figure 10. Remarkably, all four classes exhibit a similar pattern: the average speed initially increases until reaching a peak, followed by a gradual decline to a nonzero value, around which it fluctuates. Nevertheless, the peak in average speed is most pronounced for the agitated class, followed by the panic flight class, and then the adapted class. The stupor class consistently displays the lowest speed.

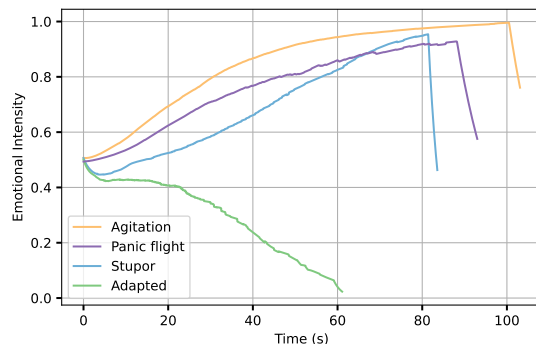


Figure 9 Changes in the overall intensity of emotions over time for each class.

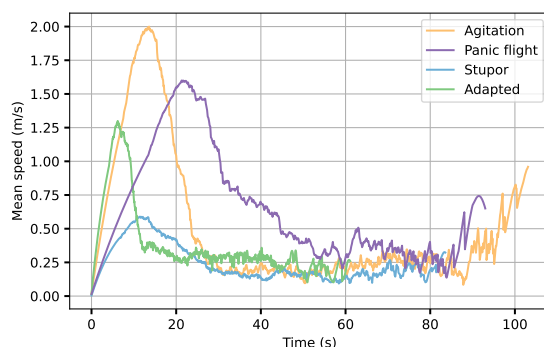


Figure 10 Changes in the mean speed over time for each class.

Specifically, individuals in the agitated class tend to run in various directions, utilizing the available space to escape the intensity of their panic. Consequently, their average speed is comparatively higher than that of the panic flight class. The individuals in the panic flight class, on the other hand, oscillate between evacuating and moving away from areas with high panic levels. This behavior leads to their congregating near exits, resulting in a slowdown of their speed. In the case of the adapted class, individuals evacuate in an orderly manner while avoiding zones characterized by high population density and panic levels. This cautionary approach causes a relative deceleration in their speed, as they take the time to analyze and determine the correct direction to proceed. Finally, individuals in the stupor class exhibit a very slow speed, consistent with their psychological state of paralysis caused by their heightened panic.

5.6.3 Dispersion

Subsequently, we examine the alignment between agents' actual behavior and their intended actions. This is assessed by quantifying the dispersion of agents, which is calculated as the angle between their actual movement direction and their desired direction at each time point during the simulation. To illustrate the degree and distribution of this dispersion for each agent, figure 11 presents a box plot. In this plot, each data point

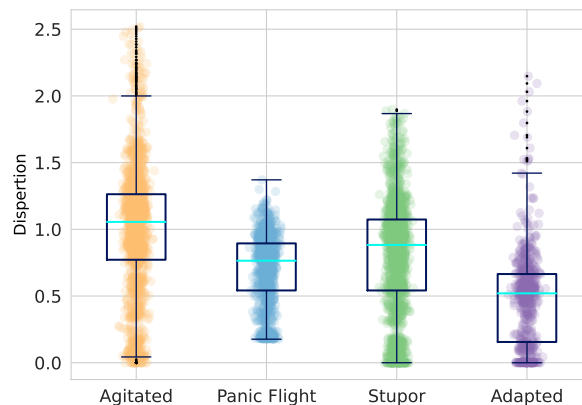


Figure 11 Box plots for each class to quantify the mean dispersion of each agent.

corresponds to the average dispersion value of each agent within his respective class.

In comparison to the adapted class, the agitated class, stupor class, and panic flight class exhibit higher levels of dispersion, with notable variations within the agitated and stupor classes. This disparity can be attributed primarily to the occurrence of collisions between agents during the evacuation process, leading to abrupt changes in direction. Agents belonging to the agitated class experience elevated levels of dispersion due to their inherent agitation, which is modeled by the introduction of random direction changes to their desired path. As a result, their movements become more brutal, leading to increased dispersion among the agents in this class. Similarly, agents in the stupor class display high levels of dispersion as they attempt to imitate the movements of their neighboring agents and adapt to their behavior. This tendency to follow others' actions contributes to a higher degree of dispersion within the stupor class.

5.6.4 Contact Forces

We interest to the pressure and the contact forces generated during collisions of pedestrians in a moving crowd. In previous works, we estimated the contact forces in dense crowds as the difference in the percussion suffered by each agent multiplied by his mass.

As depicted in Figure 12, box plots are presented, where each data point represents the average contact force experienced by individual agents within their respective classes. Agents belonging to the adapted class generally exhibit lower contact force values, as their displacement strategy involves actively avoiding close contact with other individuals. In contrast, the agitated class experiences higher contact forces due to the collisions resulting from their agitated state. The panic flight class tends to gather near exits in an attempt to escape from potential danger, leading to elevated contact forces. Similarly, the stupor class encounters moderate contact forces, as they tend to remain surrounded by the crowd rather than actively avoiding contact.

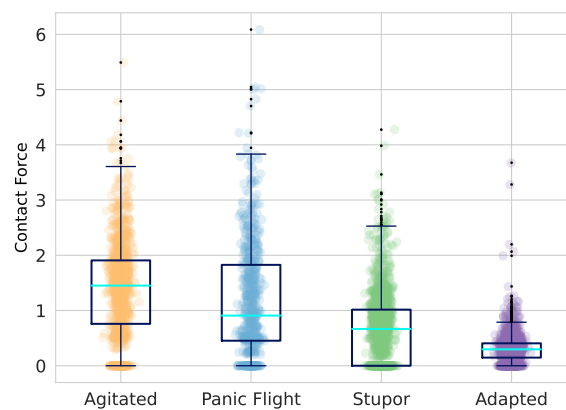


Figure 12 Box plots for each class to quantify the mean contact forces applied to each agent.

5.6.5 Evacuation Time

Evacuation time plays a critical role in evaluating the efficiency and effectiveness of crowd evacuation, serving as a crucial indicator. The bar plot depicted in figure 13 illustrates the evacuation time for different crowd densities across the four classes.

Across all densities, a consistent pattern emerges. Firstly, the agitation class exhibits the highest evacuation time. This can be attributed to the agitated nature of individuals in this class, as they tend to run in multiple directions. Their erratic behavior leads to a prolonged evacuation process. Similarly, the panic flight class demonstrates a significant evacuation time. Individuals in this class prioritize their own safety above all else, resulting in a rush to evacuate. Consequently, congestion arises, retarding the overall evacuation process. In contrast, the stupor class experiences a relatively slower evacuation process. Agents in this class are unable to move at high speeds due to their impaired state. Consequently, their evacuation time is also prolonged. Lastly, the adapted class agents display the most efficient evacuation process. Their rational decision-making during evacuation allows for a smoother flow. As a result, their evacuation time is significantly lower compared to the other classes.

5.7 Heterogeneous crowd behaviour

Having examined the overall response of people in similar crowds during panic situations, our investigation now shifts towards gaining a deeper understanding of collective behavior within a heterogeneous crowd. This particular crowd consists of individuals belonging to all four classes previously identified.

In the previous section, the study revealed a notable distinction between two classes of individuals in terms of their behaviors during evacuations: the agitated class, displaying highly intense emotions and reactive tendencies such as dispersion and contact force, and the adapted class, characterized by more rational behavior. Due to the complexity of studying the influence of all four classes on the evacuation process, we have chosen to

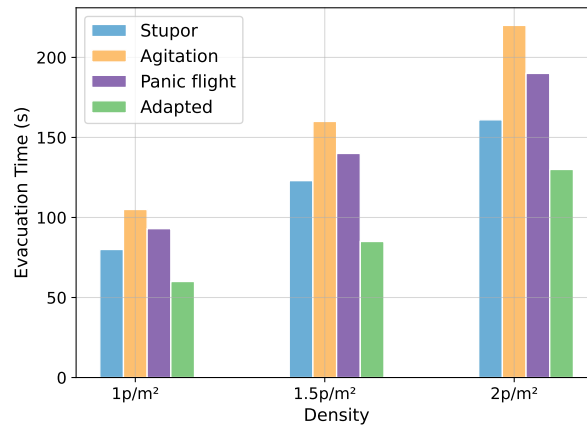


Figure 13 Bar plot of the evacuation time for different crowd densities across the four classes.

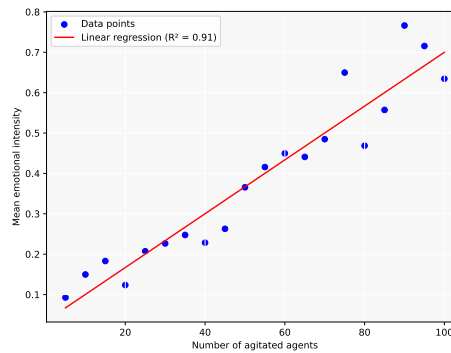


Figure 14 Emotional response of the crowd while varying the number of agitated class agents: the blue points refer to the mean emotional value while the red line is the model fitting all points due to linear regression.

focus our investigation exclusively on the agitated and adapted classes.

Initially, we consider a crowd comprising of n_1 agents from the agitated class, n_2 agents from the adapted class, n_3 agents from the stupor class, and n_4 agents from the panic flight class. Subsequently, we measure the emotional responses manifested by the crowd while varying the number of agitated class agents, as illustrated in figure 14. The blue data points correspond to the mean emotional values obtained from 10 experimental trials, while the red line is the corresponding linear regression fit. The regression line, exhibiting an R-squared value of 0.91, indicative of a good fitting of the model on the data points, effectively captures the observed trend of increasing emotional intensity as the population of agitated class agents within the crowd rises. In essence, the presence of agitated class agents significantly amplifies the overall sense of panic within the crowd.

Next, we turn our attention to investigating the interplay between the agitated class and the adapted class within the crowd. To facilitate this study, we adopt a percentage-based perspective, representing the proportion of the agitated class as p_{ag} and the proportion of

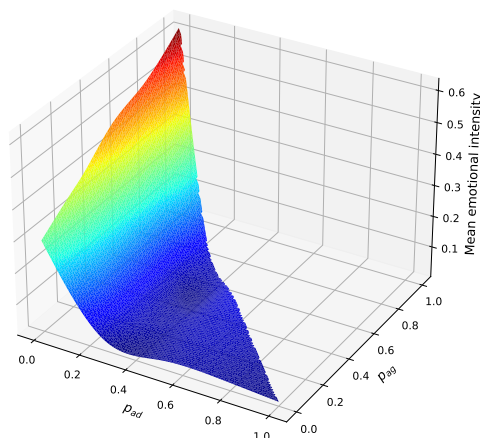


Figure 15 Crowd emotional response for different combinations of agitated class and adapted class proportions.

the adapted class as p_{ad} . To simplify our analysis, we make the assumption that given percentages p_{ag} and p_{ad} , the remaining portion of the crowd is evenly divided between the stupor and panic flight classes. Consequently, the percentages of these two classes are identical and equal to $(1 - p_{ag} - p_{ad})/2$. By employing this simplified assumption, we explore the emotional response of the crowd while simultaneously varying both p_{ag} and p_{ad} . The outcomes of this investigation are presented in figure 15, presenting the effect of different combinations of agitated class and adapted class proportions on the crowd's emotional response. The plot supports our earlier observation reaffirming that an increase in the proportion of the agitated class leads to a heightened overall emotional intensity within the crowd. Conversely, an increase in the proportion of the adapted class strongly influences a reduction in emotional intensity, meaning that the presence of the adapted class exerts a calming effect on agents from other classes.

The results underscore the vital significance of the adapted class, which serves as a mechanism for minimizing the detrimental consequences that may arise from panic situations. This role aligns directly with the role of security agents, who play a crucial part in upholding order and instilling a sense of security and assurance among individuals. The finding highlights the importance of having well-trained professionals who possess the expertise to efficiently oversee and direct crowds during emergency situations.

5.8 Comparison with other models

In the current phase of our research, we intend to conduct a comparative analysis of our model against established models in the field. Our primary focus is on contrasting our model with the original SFM outlined by Helbing [4]. This comparison is pivotal, given that our model is an extension of the original SFM framework. Additionally, we compare our model with the Improved Social Force Model Based on Emotional Contagion and Evacuation Assistant (ecaSFM) presented by Zheng et al. [16]. This model is particularly relevant for comparison due to its incorporation of multiple evacuation strategies and the integration of the assistant's category, which closely aligns with the adapted class in our model.

For an effective and comprehensive comparison, we align the configuration settings of our model to match those used in [16]. Specifically, we simulate an environment replicating a room with the size of $80\text{m} \times 50\text{m}$ with a 2m wide exit. The parameter values of SFM used in [16] are identical to those used in our model.

The initial metric for comparison is the evacuation time. Figure 16 illustrates the evacuation time for the two models as well as for the different classes of our model, and that for different population sizes, varying from 100 to 500 individuals. The results align closely with the findings from subsection 5.6.5. Particularly, the adapted class in our model surpasses both the original SFM and the ecaSFM in terms of evacuation efficiency. This improvement becomes particularly noticeable in scenarios involving large-scale crowd evacuations, such as with 500 individuals. In these cases, our model shows a 35.8% optimization in evacuation time over the original SFM, and a 17.2% improvement compared to the ecaSFM. The key factor contributing to this enhanced performance is the diversity of evacuation strategies incorporated into this class. This variety effectively reduces the occurrence of bottlenecks, a common issue when the entire crowd attempts to evacuate simultaneously. By facilitating more dynamic movement patterns, our model significantly improves overall evacuation efficiency.

Furthermore, the ecaSFM has demonstrated the positive impact of assistance on enhancing evacuation efficiency. This aligns with our findings presented earlier (section 5.7), where we established that the inclusion of the adapted class significantly mitigates the crowd's emotional response. This reduction in emotional intensity implicitly contributes to more efficient evacuation processes.

6 Conclusion

This paper presents a coupled SFM-ASCRIBE model to understand the dynamics of panicked crowds and focuses on two key objectives: examining the influence of emotions on crowd movement and gaining valuable insights into collective behavior within crowds. To accomplish these objectives, a coupled model is proposed, combining an enhanced ASCRIBE model with an agent displacement model. Heterogeneity is introduced into our model by incorporating specific mobility laws for different categories of panicked crowds, considering the impact of emotions on both speed and direction of crowd movement.

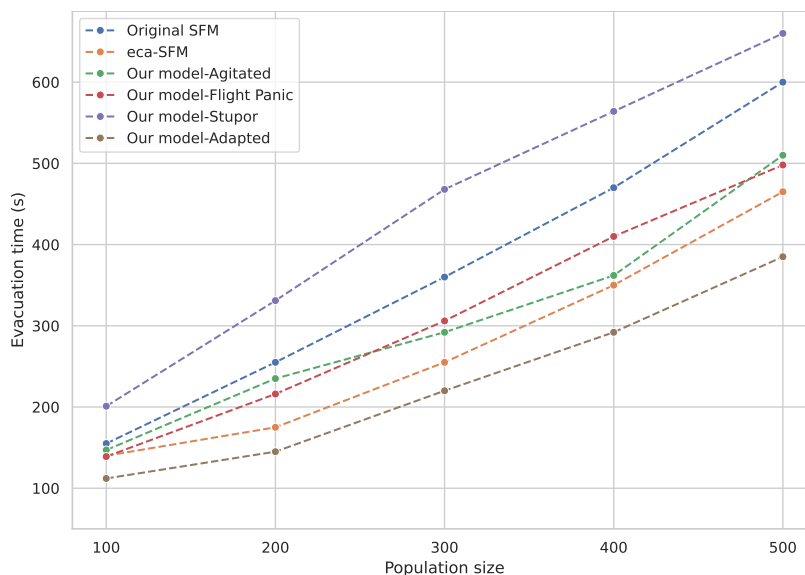


Figure 16 Comparison of evacuation time for the original SFM, ecaSFM, and our the different classes of our model, and for different population sizes, varying from 100 to 500 individuals

By conducting numerical simulations, we examine various parameters of our model, such as resilience and desired speed. We study the impact that environmental factors and geometric configurations have on the spread of emotions. Findings illustrate that the physical layout of a space, such as its dimensions and structural design, plays a crucial role in shaping how emotions propagate among individuals within that environment. This effect is particularly evident in scenarios where space constraints or design elements influence movement, interaction, and ultimately, the emotional dynamics of a group. We observe the behavior of homogeneous crowds composed of different classes of panicked individuals and explore the collective dynamics within heterogeneous crowds. The results indicate that the presence of agitated class agents greatly amplifies the overall panic intensity within the crowd, while an increase in the proportion of the adapted class results in a heightened overall panic intensity among the crowd. These findings highlight the crucial importance of the adapted class, which acts as a mechanism for minimizing the harmful consequences that can arise from panic situations. To effectively manage a panic situation, it is advisable to ensure prompt intervention by security agents to effectively manage the situation and control agitated individuals, displaying high energy levels and engaging in large gestures.

References

- [1] Üsten, E., Lügering, H., Sieben, A.: Pushing and non-pushing forward motion in crowds: A systematic psychological observation method for rating individual behavior in pedestrian dynamics. *Collective dynamics* **7**, 1–16 (2022). [doi:10.17815/CD.2022.138](https://doi.org/10.17815/CD.2022.138)

- [2] Liddle, J., Seyfried, A., Steffen, B., Klingsch, W., Rupperecht, T., Winkens, A., Boltès, M.: Microscopic insights into pedestrian motion through a bottleneck, resolving spatial and temporal variations. *Collective dynamics* **7**, 1–23 (2022). doi:[10.17815/CD.2022.139](https://doi.org/10.17815/CD.2022.139)
- [3] Gayathri, H., Gulhare, S., Verma, A.: Characteristics of stop and go wave in one dimensional interrupted pedestrian flow through narrow channel. *Collective dynamics* **3**, 1–14 (2018). doi:[10.17815/CD.2018.18](https://doi.org/10.17815/CD.2018.18)
- [4] Helbing, D., Molnár, P.: Social force model for pedestrian dynamics. *Ann Solid Struct Mech* **51(5)**, 4282–4286 (1995). doi:[10.1103/PhysRevE.51.4282](https://doi.org/10.1103/PhysRevE.51.4282)
- [5] Kirchner, A., Schadschneider, A.: Simulation of evacuation processes using a bionics-inspired cellular automaton model for pedestrian dynamics. *Physica A: statistical mechanics and its applications* **312(1-2)**, 260–276 (2002). doi:[10.1016/S0378-4371\(02\)00857-9](https://doi.org/10.1016/S0378-4371(02)00857-9)
- [6] Muramatsu, M., Irie, T., Nagatani, T.: Jamming transition in pedestrian counter flow. *Physica A: Statistical Mechanics and its Applications* **267(3-4)**, 487–498 (1999). doi:[10.1016/S0378-4371\(99\)00018-7](https://doi.org/10.1016/S0378-4371(99)00018-7)
- [7] Ma, L., Chen, B., Wang, X., Zhu, Z., Wang, R., Qiu, X.: The analysis on the desired speed in social force model using a data driven approach. *Physica A: Statistical Mechanics and its Applications* **525**, 894–911 (2019). doi:[10.1016/j.physa.2019.03.087](https://doi.org/10.1016/j.physa.2019.03.087)
- [8] Frémond, M.: Rigid bodies collisions. *Physics Letters A* **204(1)**, 33–41 (1995). doi:[10.1016/0375-9601\(95\)00418-3](https://doi.org/10.1016/0375-9601(95)00418-3)
- [9] Jebrane, A., Argoul, P., Hakim, A., Rhabi, M.E.: Estimating contact forces and pressure in a dense crowd: Microscopic and macroscopic models. *Applied Mathematical Modelling* **74**, 409–421 (2019). doi:[10.1016/j.apm.2019.04.062](https://doi.org/10.1016/j.apm.2019.04.062)
- [10] Pécol, P., Pont, S.D., Erlicher, S., Argoul, P.: Smooth/non-smooth contact modeling of human crowds movement: numerical aspects and application to emergency evacuations. *Annals of Solid and Structural Mechanics* **2**, 62–85 (2011). doi:[10.1007/s12356-011-0019-3](https://doi.org/10.1007/s12356-011-0019-3)
- [11] Helbing, D., Farkas, I., Vicsek, T.: Simulating dynamical features of escape panic. *Nature* **407(6803)**, 487–490 (2000). doi:[10.1038/35035023](https://doi.org/10.1038/35035023)
- [12] Fu, L., Song, W., Lv, W., Liu, X., Lo, S.: Multi-grid simulation of counter flow pedestrian dynamics with emotion propagation. *Simulation Modelling Practice and Theory* **60**, 1–14 (2016). doi:[10.1016/j.simpat.2015.09.007](https://doi.org/10.1016/j.simpat.2015.09.007)
- [13] Cao, M., Zhang, G., Wang, M., Lu, D., Liu, H.: A method of emotion contagion for crowd evacuation. *Physica A: Statistical Mechanics and its Applications* **483**, 250–258 (2017). doi:[10.1016/j.physa.2017.04.137](https://doi.org/10.1016/j.physa.2017.04.137)

- [14] Cornes, F., Frank, G., Dorso, C.O.: Fear propagation and the evacuation dynamics. *Simulation Modelling Practice and Theory* **95**, 112–133 (2019). [doi:10.1016/j.simpat.2019.04.012](https://doi.org/10.1016/j.simpat.2019.04.012)
- [15] Xu, M., Li, C., Lv, P., Chen, W., Deng, Z., Zhou, B., Manocha, D.: Emotion-based crowd simulation model based on physical strength consumption for emergency scenarios. *IEEE Transactions on Intelligent Transportation Systems* (2020). [doi:10.1109/TITS.2020.3000607](https://doi.org/10.1109/TITS.2020.3000607)
- [16] Zheng, Z., Zhu, G., Sun, Z., Wang, Z., Li, L.: Improved social force model based on emotional contagion and evacuation assistant. *IEEE Access* **8**, 195989–196001 (2020). [doi:10.1109/ACCESS.2020.3034348](https://doi.org/10.1109/ACCESS.2020.3034348)
- [17] Zhou, R., Ou, Y., Tang, W., Wang, Q., Yu, B.: An emergency evacuation behavior simulation method combines personality traits and emotion contagion. *Ieee Access* **8**, 66693–66706 (2020). [doi:10.1109/ACCESS.2020.2985987](https://doi.org/10.1109/ACCESS.2020.2985987)
- [18] Mao, Y., Fan, Z., Zhao, J., Zhang, Q., He, W.: An emotional contagion based simulation for emergency evacuation peer behavior decision. *Simulation Modelling Practice and Theory* **96**, 101936 (2019). [doi:10.1016/j.simpat.2019.101936](https://doi.org/10.1016/j.simpat.2019.101936)
- [19] Liu, T.T., Liu, Z., Ma, M., Xuan, R., Chen, T., Lu, T., Yu, L.: An information perception-based emotion contagion model for fire evacuation. *3D Research* **8**, 1–16 (2017). [doi:10.1007/s13319-017-0120-4](https://doi.org/10.1007/s13319-017-0120-4)
- [20] Cao, R.F., Lee, E.W.M., Yuen, A.C.Y., Chan, Q.N., Xie, W., Shi, M., Yeoh, G.H.: Development of an evacuation model considering the impact of stress variation on evacuees under fire emergency. *Safety science* **138**, 105232 (2021). [doi:10.1016/j.ssci.2021.105232](https://doi.org/10.1016/j.ssci.2021.105232)
- [21] Xu, T., Shi, D., Chen, J., Li, T., Lin, P., Ma, J.: Dynamics of emotional contagion in dense pedestrian crowds. *Physics Letters A* **384**(3), 126080 (2020). [doi:10.1016/j.physleta.2019.126080](https://doi.org/10.1016/j.physleta.2019.126080)
- [22] Mao, Y., Fan, X., Fan, Z., He, W.: Modeling group structures with emotion in crowd evacuation. *IEEE Access* **7**, 140010–140021 (2019). [doi:10.1109/ACCESS.2019.2943603](https://doi.org/10.1109/ACCESS.2019.2943603)
- [23] Mao, Y., Yang, S., Li, Z., Li, Y.: Personality trait and group emotion contagion based crowd simulation for emergency evacuation. *Multimedia Tools and Applications* **79**, 3077–3104 (2020). [doi:10.1007/s11042-018-6069-3](https://doi.org/10.1007/s11042-018-6069-3)
- [24] Xiao, Q., Li, J.: Pedestrian evacuation model considering dynamic emotional update in direction perception domain. *Complexity* **2021**, 1–16 (2021). [doi:10.1155/2021/5530144](https://doi.org/10.1155/2021/5530144)

- [25] Li, F., Chen, S., Wang, X., Feng, F.: Pedestrian evacuation modeling and simulation on metro platforms considering panic impacts. *Procedia-social and behavioral sciences* **138**, 314–322 (2014). doi:[10.1016/j.sbspro.2014.07.209](https://doi.org/10.1016/j.sbspro.2014.07.209)
- [26] Niu, Y., Chen, Y., Kong, D., Yuan, B., Zhang, J., Xiao, J.: Strategy evolution of panic pedestrians in emergent evacuation with assailants based on susceptible-infected-susceptible model. *Information Sciences* **570**, 105–123 (2021). doi:[10.1016/j.ins.2021.04.040](https://doi.org/10.1016/j.ins.2021.04.040)
- [27] Guo, X., Chen, J., Zheng, Y., Wei, J.: A heterogeneous lattice gas model for simulating pedestrian evacuation. *Physica A: Statistical Mechanics and its Applications* **391**(3), 582–592 (2012). doi:[10.1016/j.physa.2011.07.055](https://doi.org/10.1016/j.physa.2011.07.055)
- [28] Hrabák, P., Bukáček, M.: Influence of agents heterogeneity in cellular model of evacuation. *Journal of computational science* **21**, 486–493 (2017). doi:[10.1016/j.jocs.2016.08.002](https://doi.org/10.1016/j.jocs.2016.08.002)
- [29] Li, Y., Chen, M., Zheng, X., Dou, Z., Cheng, Y.: Relationship between behavior aggressiveness and pedestrian dynamics using behavior-based cellular automata model. *Applied Mathematics and Computation* **371**, 124941 (2020). doi:[10.1016/j.amc.2019.124941](https://doi.org/10.1016/j.amc.2019.124941)
- [30] Wu, W., Chen, M., Li, J., Liu, B., Zheng, X.: An extended social force model via pedestrian heterogeneity affecting the self-driven force. *IEEE Transactions on Intelligent Transportation Systems* **23**(7), 7974–7986 (2022). doi:[10.1109/TITS.2021.3074914](https://doi.org/10.1109/TITS.2021.3074914)
- [31] Wu, W., Li, J., Yi, W., Zheng, X.: Modeling crowd evacuation via behavioral heterogeneity-based social force model. *IEEE Transactions on Intelligent Transportation Systems* **23**(9), 15476–15486 (2022). doi:[10.1109/TITS.2022.3140823](https://doi.org/10.1109/TITS.2022.3140823)
- [32] Kabalan, B., Argoul, P., Jebrane, A., Cumunel, G., Erlicher, S.: A crowd movement model for pedestrian flow through bottlenecks. *Ann Solid Struct Mech* **8**, 1–15 (2016). doi:[10.1007/s12356-016-0044-3](https://doi.org/10.1007/s12356-016-0044-3)
- [33] Jebrane, A., Argoul, P., Hakim, A., Rhabi, M.E.: Estimating contact forces and pressure in a dense crowd: Microscopic and macroscopic models. *Applied Mathematical Modelling* **74**, 409–421 (2019). doi:[10.1016/j.apm.2019.04.062](https://doi.org/10.1016/j.apm.2019.04.062)
- [34] Cao, M., Zhang, G., Wang, M., Lu, D., Liu, H.: A method of emotion contagion for crowd evacuation. *Physica A: Statistical Mechanics and its Applications* **483**, 250–258 (2017). doi:[10.1016/j.physa.2017.04.137](https://doi.org/10.1016/j.physa.2017.04.137)
- [35] Crocq, L.: Secours psychologiques aux victimes d’attentats terroristes: Partie 1: Tableaux cliniques relatifs aux attentats de 1986 et 1995 (2016). doi:[10.1051/ppsyp/2016554253](https://doi.org/10.1051/ppsyp/2016554253)

- [36] Pecol, P.: Modélisation 2d discrète du mouvement des piétons: application à l'évacuation des structures du génie civil et à l'interaction foule-passerelle. Ph.D. thesis, Université Paris-Est (2011)
- [37] Xiao, Y., Gao, Z., Qu, Y., Li, X.: A pedestrian flow model considering the impact of local density: Voronoi diagram based heuristics approach. *Transportation research part C: emerging technologies* **68**, 566–580 (2016). [doi:10.1016/j.trc.2016.05.012](https://doi.org/10.1016/j.trc.2016.05.012)
- [38] Lakoba, T.I., Kaup, D.J., Finkelstein, N.M.: Modifications of the helbing-molnar-farkas-vicsek social force model for pedestrian evolution. *Simulation* **81**(5), 339–352 (2005). [doi:10.1177/0037549705052772](https://doi.org/10.1177/0037549705052772)